PYROELECTRIC RESPONSE AND FIGURES OF MERIT OF LEAD-FREE FERROELECTRIC CERAMICS

RESPUESTA PIROELÉCTRICA Y FIGURAS DE MÉRITO DE CERÁMICAS FERROELÉCTRICAS LIBRES DE PLOMO

A. C. Iglesias-Jaime[a], A. Peláiz-Barranco[a,b,c†], J. D. S. Guerra[c], Tongqing Yang[b]

a) Grupo de Materiales Ferroicos, Facultad de Física–IMRE, Universidad de la Habana. San Lázaro y L, Vedado. La Habana 10400, Cuba. pelaiz@física.uh.cu†
b) Functional Materials Research Laboratory, School of Materials Science and Engineering, Tongji University, 4800 Cao'an Road, Shanghai 201804, China.
c) Grupo de Ferroeléctricos Multifuncionais, Instituto de Física, Universidade Federal de Uberlândia, Minas Gerais, 38408-100, Brazil.
† corresponding author

Recibido 4/2/2025; Aceptado 26/3/2025

Keywords: Ferroelectrics (ferroeléctricos); pyroelectrics (piroeléctricos); pyroelectric devices (dispositivos piroeléctricos).

I. INTRODUCTION

Lead-free ferroelectric materials have been extensively studied as a quest to replace lead-based ferroelectric commonly used in engineering systems such as actuators, batteries, sonars, sensors, electromechanic engines, etc [1–3]. Numerous authors have conducted research on various aspects of the ferroelectric, dielectric and piezoelectric properties. However, there not many studies specifically addressing its pyroelectric behavior [4, 5].

The $(Bi_{0.5}Na_{0.5})_{1-x}Ba_xTiO_3$ (BNT-xBT) system has been reported as one of the most promising materials to replace the lead-based systems, receiving a growing interest from the scientific society [2, 6–10], but with only a few publications regarding its pyroelectric behavior [6–8]. The main pyroelectric investigations of the BNT-xBT have been centered on the morphotropic phase boundary (MPB), around x = 0.06 *at* %, and have involved doping with elements such as tantalum, zirconium and manganese in order to enhance the pyroelectric properties [6–8].

Recently, $(Bi_{0.5}Na_{0.5})_{1-x}Ba_xTiO_3$ lead-free ferroelectric ceramics (x = 0, 2, 5, 8, 10, 12, 16, 18 *at* %) were studied considering x-ray diffraction, Raman spectroscopy, dielectric and piezoelectric behavior [9, 10]. From these results, a new phase diagram has been proposed considering a wider compositional range than those reported in the literature, which offers new insights for a better understanding on the features of the phase diagram for the ceramic system [9]. Also, very good piezoelectric parameters were reported for composition showing tetragonal phases [10]. From this point of view, the two highest barium concentrations have been selected in order to evaluate the pyroelectric behavior in a wide temperature range. It is known that depending on the specific application, selecting an optimal pyroelectric material becomes crucial to achieve maximum efficiency in pyroelectric devices. In this sense, the evaluation of several parameters, such as the figures of merit (FOMs) is very important [11], which guide us toward the most suitable material for the intended purpose. Generally, FOMs are described by four characteristic parameters known as current responsivity (F_i), voltage responsivity (F_V), detectivity (F_D) and the energy harvesting figure of merit (F_E), as expressed by the equations (1) to (4), respectively [11, 12].

$$F_i = \frac{p}{\rho C_p} \tag{1}$$

$$F_V = \frac{p}{\rho C_p \varepsilon_0 \varepsilon} \tag{2}$$

$$F_D = \frac{p}{\rho C_p \sqrt{\varepsilon_0 \varepsilon \tan\delta}} \tag{3}$$

$$F_E = \frac{p^2}{\varepsilon_0 \varepsilon} \tag{4}$$

F_i characterizes the maximum current that can be generated, F_V represents the maximum voltage output of the sample, F_D provides the voltage responsivity with the optimal signal-to-noise ratio and F_E characterizes the capacity for energy harvesting from temperature change [13, 14]. The p parameter corresponds to the pyroelectric coefficient, ρ represents the density, C_p is the specific heat at constant pressure, ε denotes the dielectric permittivity, and $\tan\delta$ represents the dielectric losses of the material [15].

In this context, the objective of the present paper is to evaluate the pyroelectric response and the corresponding figures of merit for $(Bi_{0.5}Na_{0.5})_{1-x}Ba_xTiO_3$ (x=16 and 18 *at* %) ceramic system.

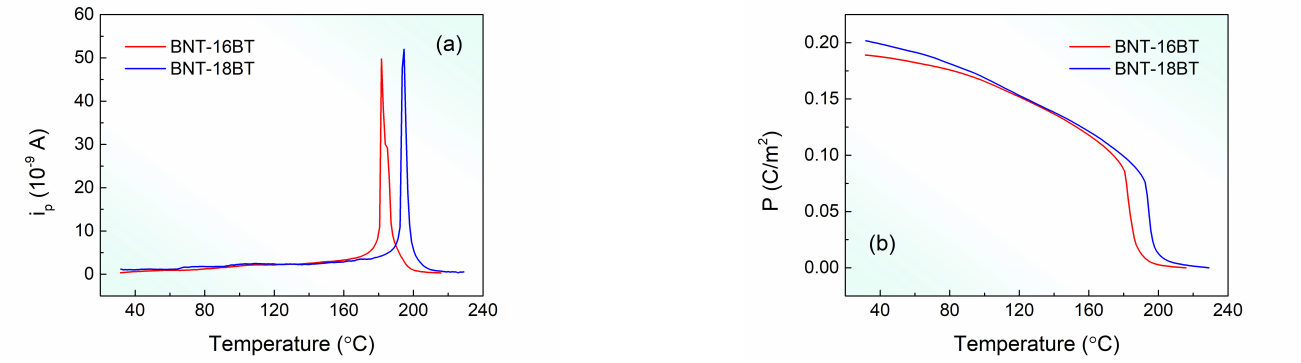

Figure 1. Temperature dependence of (a) pyroelectric current (i_p) and (b) remnant polarization (P), for the studied samples.

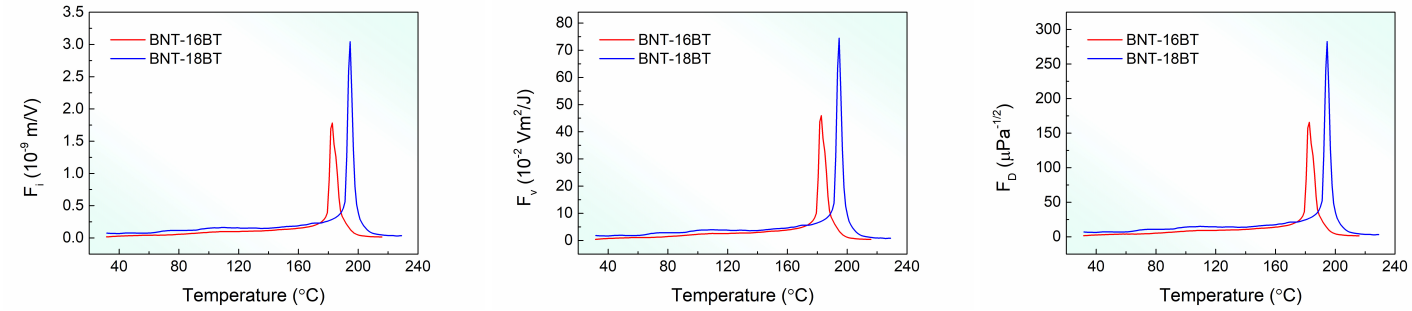

Figure 2. Temperature dependence of the FOMs for the studied samples.

II. EXPERIMENTAL PROCEDURE

$(Bi_{0.5}Na_{0.5})_{1-x}Ba_xTiO_3$ ceramics, for x = 16 and 18 *at* %, were prepared by using the solid-state reaction sintering method. High purity oxides (Bi_2O_3: 99.999 %; Ba_2CO_3: 99.36 %; Ti_2O_2: 98 %; Na_2CO_3: 99.5 %) were mixed and manually milled using a mortar for 2 hours. The samples were calcinated at 800 °C for 1 hour in air atmosphere. The powders were milled again and pressed as thin discs by using 2 ton/cm^2. The disc ceramics were sintered at 1150 °C for 2 hours in an air atmosphere, using a covered platinum crucible to prevent bismuth loss through evaporation. The samples were hereafter labeled as BNT-16BT and BNT-18BT, respectively. The structural analysis confirmed the formation of a pure perovskite structure without additional spurious phases, showing a tetragonal phase [9].

Silver paint electrodes were applied on the opposite parallel surfaces of disk-shaped ceramics samples by a heat treatment at 590 °C. The polarization process was carried out at 100 °C, applying an electric field of 2 kV/mm. Once polarized the samples, the pyroelectric current (i_p) was directly measured through the static method using a Keithley 6485 Picoammeter covering a wide temperature range (25 – 210 °C). The remnant polarization (P) and the pyroelectric coefficient were calculated from the temperature dependence of i_p [16]. The temperature dependence of the pyroelectric figures of merit (FOMs) were obtained by using Eqs. (1), (2), (3) and (4), as well as the dielectric parameters reported elsewhere [9].

III. RESULTS AND CONCLUSIONS

Figure 1 shows the temperature dependence of the pyroelectric current (i_p) and the remnant polarization (P) for the studied compositions. A typical peak for the pyroelectric current around 180 - 200 °C has been obtained for both samples, with the corresponding decreasing to zero at the reported depolarization temperature (T_d) [9]. It is important to note the high thermal stability through the studied temperature range, which is a relevant behavior to be consider for applications involving high-temperature sensors [17].

Figure 2 shows the temperature dependence for the corresponding FOMs, given by equations (1), (2) and (3). The behavior is similar to that obtained for the pyroelectric current (T_d) [9], with well-defined peaks below the depolarization temperature and also high thermal stability. The maximum obtained values for the FOMs, located near around this critical temperature, are higher than those for other reported materials, such as $BaCe_{0.12}Ti_{0.88}O_3$ [18], $Ba_{0.85}Ca_{0.15}Zr_{0.1}Ti_{0.9}O_3$ [19] and $PbNb_{0.02}(Zr_{0.95}Ti_{0.05})_{0.98}O_3$ [20], which were even polarized at higher electric fields than the studied ceramics.

Table 1 summarizes the obtained values of the FOMs from Figure 2, at room temperature, of the studied samples and other ceramic systems reported in the literature. It can be observed that F_i values of both studied samples are quite modest in comparison with the literature average, which can be attributed to the low p values obtained. The BNT-18BT shows better results than those of BNT-16BT, being the F_V

parameter which exhibit the best result, representing the maximum voltage output that can be obtained from the sample.

The most relevant result which has been obtained in the present study corresponds to the F_E parameter, in particular for BNT-18BT. Figure 3 shows this FOM at room temperature for several reported materials, included the studied compositions, suggesting the suitability of BNT-18BT for pyroelectric energy harvesting (PyEH) [28]. This high F_E value is mostly attributed to the low permittivity value of this sample at room temperature [10].

Table 1. FOMs at room temperature for the studied compositions and other reported ceramic systems.

Materials	$\mathbf{F_i}$ (10^{-9} mV)	$\mathbf{F_V}$ (10^{-2} m^2/C)	$\mathbf{F_D}$ (μPa$^{-0.5}$)
BNT-16BT	0.02	0.42	1.5
BNT-18BT	0.07	1.8	6.8
BCT 21 [21]	1.71	0.9	-
BNT-BT-ST [22]	-	1.8	5.89
BTS [23]	1.03	0.2	-
BCSZT [5]	3.86	1.7	28.4
BNKLBTT [24]	2.21	3.0	14.8
BNT-BTZ [7]	2.03	2.2	10.5
PLZT-25 [25]	1.10	4.4	50.1
PLZT-50 [25]	0.12	0.16	1.9
PLZT 4/86/14 [26]	2.90	4.8	35.4
PLZT-0.11Cr [27]	1.55	1.16	8.3

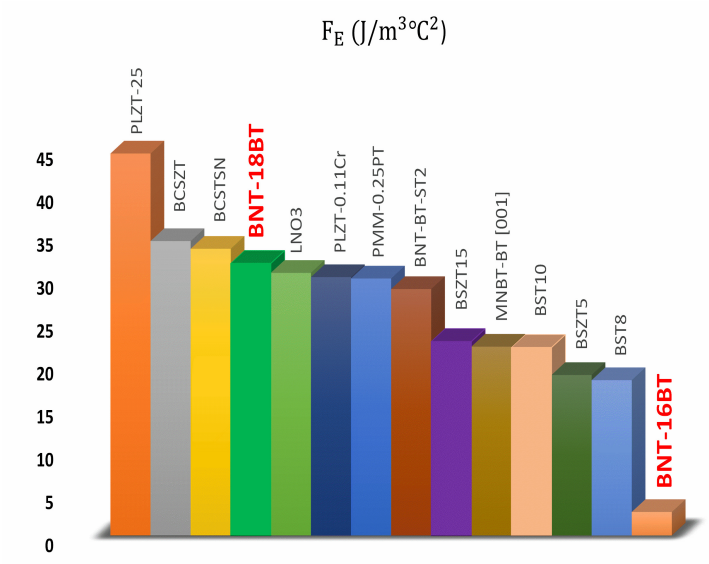

Figure 3. F_E values at room temperature for the studied samples, BNT-16BT and BNT-18BT, and other previous reported materials. PLZT-25 [25], BCSZT [5], BCSTSN [29], LNO3 [15], PLZT-0.11Cr [27], PMN-0.25PT [12], BNT-BT-ST2 [22], BSZT15 [30], MNBT-BT [001] [31], BTS10 [32], BSZT5 [30], BST8 [32].

From this point of view and considering the previous piezoelectric results [10] for the studied BNT-18BT, this compound emerges as an excellent candidate for energy harvesting applications based in the pyroelectric, piezoelectric effect or their combination.

IV. ACKNOWLEDGEMENTS

The authors acknowledge the National Council of Scientific and Technological Development (CNPq) Grants (Nos. 303447/2019-2, 309494/2022-2 and 408662/2023-9), Minas Gerais Research Foundation (FAPEMIG) Grants (Nos. PPM-00661-16 and APQ-02875-18), Coordenação de Aperfeiçoamento de Pessoal de Nível Superior—Brasil (CAPES)—Finance Code 001 and PROAP/CAPES—AUXPE 0237/2021 (UNESP—Ilha Solteira, So Paulo) from Brazil, for the financial support. Special thanks to ICTP for financial support of Latin-American Network of Ferroelectric Materials (NT-02). Thanks to the National Program for Basic Sciences of Cuba (Project No. PN223LH010-068) and the National Program for Nanoscience and Nanotechnology (Project No. PN211LH008-069). This work was supported by the National Key R&D Program of China (No. 2023YFE0198300).

REFERENCES

[1] K. Uchino, *Lead-Free Piezoelectrics*, Eds. S. Priya and S. Nahm, Chapter 17 (Springer, New York, 2012), pp. 511.
[2] I. Coondoo, N. Panwar and A. Kholkin, *J. Adv. Dielect.* **3**, 1330002 (2013).
[3] S. Supriya, *Coord. Chem. Rev.* **479**, 215010 (2023).
[4] R. W. Whatmore, *J. Appl. Phys.* **133**, 080902 (2023).
[5] H. He. X. Liu. E. Hanc, C. Chen, H. Zhang and L. Lu, *J. Mat. Chem. C* **8**, 1494 (2020).
[6] A. Balakt, C. Shaw and Q. Zhang, *Ceram. Int.* **43**, 3726 (2017).
[7] F. Guo, B. Yang, S. Zhang, F. Wu, D. Liu, P. Hu, Y. Sun, D. Wang and W. Cao, *Appl. Phys. Lett.* **103**, 182906 (2013).
[8] J. Abe, M. Kobune, T. Nishimura, T. Yazaw and Y. Nakai, *Integr. Ferroel.* **80**, 87 (2006).
[9] B. R. Moya, A. C. Iglesias-Jaime, A. C. Silva, A. Peláiz-Barranco and J. D. S. Guerra, *J. Appl. Phys.* **135**, 164106 (2024).
[10] A. C. Iglesias-Jaime, T. Yang. A. Peláiz-Barranco and J. D. S. Guerra, *Rev. Cub. Fis.* **39**, 33 (2022).
[11] H. Li, C. Bowen and Y. Yang, *Adv. Funct. Mater.* **31**, 2100905 (2021).
[12] C. R. Bowen, J. Taylor, E. LeBoulbar, D. Zabek, A. Chauhan and R. Vaish, *Energy Environ. Sci.* **7**, 3836 (2014).
[13] D. Zhang, H. Wu, C. R. Bowen and Y. Yang, Small **17**, 2103960 (2021).
[14] S. B. Land and D. K. Das-Gupta, *Handbook of advanced electronic and photonic materials and devices*, Chapter 1 (Academic Press, 2001).
[15] S. B. Lang, *Phys. Today* **58**, 31 (2005).
[16] S. B. Lang, *Source Book of Pyroelectricity* (Gordon and Breach, Chience Publishers Inc., New York, 1974).
[17] X. Jian, K. Kim, S. Zhang, J. Johnson and G. Salazar, *Sensors* **14**, 144 (2014).
[18] S. M. Zeng, X. G. Tang, Q. X. Liu, Y. P. Jiang, M. D. Li, W. H. Li and Z. H. Tang, *J. Alloy. Compd.* **776**, 731 (2019).
[19] M. Sharma, V. P. Singh, S. Singh, P. Azad, B. Ilahi and N. A. Madhar, *J. Electron. Mater.* **47**, 4882 (2018).
[20] H. Wei and Y. Chen, *Ceram. Int.* **41**, 6158 (2015).

[21] K. S. Srinkanth and R. Vaish, *J. Eur. Ceram. Soc.* **37**, 3927 (2017).
[22] S. Patel, A. Chauhan, S. Kundu, N. A. Madhar, B. Ilahi, R. Vaish and K. B. R. Varma, *AIP Advances* **5**, 087145 (2015).
[23] K. Srikanth, S. Patel and R. Vaish, *Int. J. Appl. Ceram. Technol.* **15**, 546 (2018).
[24] S. T. Lau, C. H. Cheng, S. H. Choy, D. M. Lin, K. W. Kwok and H. L. Chan, *J. Appl. Phys.* **103**, 104105 (2008).
[25] J. D. S. Guerra, A. Peláiz-Barranco, A. C. Silva, F. Calderón-Piñar and A. Iglesias-Jaime, *Ferroelectrics* **611**, 138 (2023).
[26] P. Qiao, Y. Zhang, X. Chen, M. Zhou, G. Wang and X. Dong, *Ceram. Int.* **45**, 7114 (2019).
[27] K. K. Bajpai, K. Sreenivas, A. K. Gupta and A. K. Shukla, *Ceram. Int.* **45**, 14111 (2019).
[28] A. Thakre, A. Kumar, S. Hyun-Cheol, J. Dae-Yong and R. Jungho, *Sensors* **19**, 2170 (2019).
[29] X. Liu, D. Xu, Z. Chen, B. Fang, J. Ding, X. Zhao and H. Luo, *Adv. Appl. Ceram.* **114**, 436 (2015).
[30] M. Aggarwal, M. Kumar, R. Syal, V. P. Singh, A. K. Singh, S. Dhiman and S. Kumar, *J. Mater. Sci. Mater. Electron.* **31**, 2237 (2020).
[31] R. Sun, J. Wang, F. Wang, T. Feng, Y. Li, Z. Chi, X. Zhao and H. Luo, *J. Appl. Phys.* **115**, 074101 (2014).
[32] K. S. Srinkanth, V. P. Singh and R. Vaish, *Int. J. Appl. Ceram. Techn.* **15**, 140 (2018).